Respiratory Physiology & Neurobiology 302 (2022) 103917

Contents lists available at ScienceDirect

Respiratory Physiology & Neurobiology

journal homepage: www.elsevier.com/locate/resphysiol

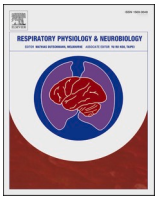

Computational fluid dynamics assessed changes of nasal airflow after inferior turbinate surgery

Jaakko Ormiskangas [a,b,*], Olli Valtonen [a,c], Teemu Harju [a,c], Markus Rautiainen [a,c], Ilkka Kivekäs [a,c]

[a] Faculty of Medicine and Health Technology, Tampere University, Tampere, Finland
[b] Faculty of Engineering and Natural Sciences, Automation Technology and Mechanical Engineering Unit, Tampere University, Tampere, Finland
[c] Department of Otorhinolaryngology – Head and Neck Surgery, Tampere University Hospital, Tampere, Finland

ARTICLE INFO

Key Words:
CBCT
CFD
Nasal cavity
Inferior turbinate
Mucous membrane

ABSTRACT

Objective: To demonstrate how Computational Fluid Dynamics (CFD) simulations can reveal important airflow changes in the nasal cavities due to surgical interventions.
Material and methods: The steady inspiratory airflow of eight patients was studied pre- and postoperatively with heat transfer from the mucous membrane by performing CFD calculations to patient specific cone beam computed tomography (CBCT) images. Eight patients with the largest distance from pre- and postoperative mean changes in inferior turbinate volumetry and Visual Analogue Scale (VAS) results were selected.
Results: Calculated CFD heat transfer results from the anterior parts of the inferior turbinates, where surgical interventions were performed, decreased significantly. The heat transfer results were in line with VAS changes.
Conclusion: Surgical interventions reduced heat transfer in the operated parts of the inferior turbinates and were in line with VAS changes. CFD is an option in assessing patient well-being as a function of airflow parameters from mucous membrane with larger data sets. The limitations of the study were the small sample size and the preliminary nature of the study.

1. Introduction

Currently, acoustic rhinometry and rhinomanometry are the most well-established objective methods for assessing nasal congestion and the nasal cavities. Unfortunately, a patient's subjective assessment of nasal congestion does not necessarily correlate with the findings of these objective methods. Another drawback is that information obtained from rhinomanometric studies is not detailed enough for the studying and planning of nasal surgeries. Acoustic rhinometry obtains a two-dimensional (2D) cross-sectional area measurement along the nasal cavities, whereas rhinomanometry obtains a global assessment of the flow. Its most commonly used form is active anterior rhinomanometry, where flow is studied separately for both sides of the nasal cavities. The separate results are then calculated together to obtain total nasal airflow resistance. An excellent review of the above methods has been published (Vogt et al., 2010). However, information obtained from rhinomanometric studies is not detailed enough for studying and planning the nasal surgeries.

Cone beam computed tomography (CBCT) imaging provides full three-dimensional (3D) information on the nasal cavities, which is not obtained in rhinomanometric studies. However, the information obtained from CBCT imaging is not used to its full extent in clinical practice. Furthermore, postoperative CBCT information from patients is scarce, as in daily practice these images are not usually gathered. The information obtained from CBCT scans can be used for CFD calculations to comprehensively study nasal airflow in the nasal cavities. In addition, CFD calculations can be used to obtain information that is useful in assessing the subjective nasal patency of patients. A literature review of these methods has been conducted (Radulesco et al., 2019). Unfortunately, CFD calculations are time-consuming and require technical expertise. Therefore, many challenges still remain for the studies of nasal airflow. These challenges have been previously described in a number of reviews (Zubair et al., 2012; Kim et al., 2013; Quadrio et al., 2014).

In the present study, we aim to demonstrate how CFD calculations can be used to study the effects of inferior turbinate surgery from CBCT

* Correspondence to: Faculty of Medicine and Health Technology, Faculty of Engineering and Natural Sciences, Automation Technology and Mechanical Engineering Unit, Tampere University, Tampere FIN-33520, Finland.
E-mail address: jaakko.ormiskangas@tuni.fi (J. Ormiskangas).

https://doi.org/10.1016/j.resp.2022.103917
Received 1 September 2021; Received in revised form 1 April 2022; Accepted 26 April 2022
Available online 29 April 2022

images acquired preoperatively and at one-year follow-up.

2. Material and methods

2.1. Surgical procedure and follow-up visit

In the present study, 8 patients from a cohort of 25 patients with chronic nasal obstruction were included. The included patients had no chronic sinusitis, nasal polyps or other pathologies. All 25 patients had enlarged inferior turbinates and had undergone radiofrequency thermal ablation (RFTA) treatment (Sutter RF generator BM-780 II, Freiburg, Germany) to the anterior parts of the inferior turbinates on both sides. The surgical process is described in detail in a study by Harju et al. (2018). The patients were evaluated prior to surgery and at one year after surgery. During both visits, patients were scanned with cone beam computed tomography (CBCT) (Planmeca Max, Planmeca, Helsinki, Finland). The following imaging parameters were used: 0.2 mm CT slice thickness, voxel size 0.2 mm, 90 kVp, 8 mA and 4 s radiation time. Additionally, patients were asked to fill out the Visual Analogue Scale (VAS) questionnaire pre- and postoperatively to assess the severity of nasal obstruction on both sides simultaneously. The VAS questionnaire assessed patient experiences from the previous 7 days. Institutional Review Board approval for the study (R13144) was obtained from Tampere University Hospital Ethics Committee, Tampere, Finland.

2.2. CBCT data and CFD calculations

Our aim was to demonstrate the use of CFD calculations in the evaluation of changes in flow variables between pre- and postoperative conditions in inferior turbinate surgery. At present, this process requires a lot of time and computational resources. Therefore, from the whole cohort of 25 patients, we chose only eight patients, who represented varying extremities of objective and subjective responses. The eight patients were subsequently divided into four groups based on air space volumetric changes surrounding the anterior 5–20 mm of the inferior turbinates between the pre- and postoperative CBCT scans and changes in VAS during the one-year follow-up. For the analysis, the groups (two patients per group) were called Group 1 (large VAS changes and large volumetric changes), Group 2 (large VAS changes and small volumetric changes), Group 3 (small VAS changes and large volumetric changes) and Group 4 (small VAS changes and small volumetric changes) (Table 1).

The CBCT data of the chosen patients were saved to a file in Digital Imaging and Communications in Medicine (DICOM) format and downloaded to OnDemand3D™ software (version 1.0, CyberMed, Inc., Yuseong-gu, Daejeon, South Korea). The software was then used to create a 3D model the air space in the nasal cavities from the nostrils to nasopharynx. For 3D modelling, Hounsfield unit (HU) values from -1000 to -430. were used to represent the air space according to previous studies (Valtonen et al., 2018; Valtonen et al., 2020; Ormiskangas et al., 2020; Valtonen et al., 2021). The maxillary, frontal and sphenoidal sinuses were excluded from the study. Additionally, any small 3D modelling artefacts included in the 3D models by the software, were manually excluded from the structures of interest. The prepared 3D models were then saved in Standard Tessellation Language (STL) format. When necessary, any small artefacts possibly still found in the 3D models, were removed from the STL files with the open-source modelling software Blender v2.82a (Blender Foundation).

The STL files were then meshed with open source OpenFOAM 5.0 software's utilities blockMesh and snappyHexMesh. The meshing of wall boundary layers was made using absolute size refinements, whereas hexahedrical elements were used for the inner geometry with similar cell sizes in all regions. Mesh sizes were between four and six million cells in all calculations.

The same OpenFOAM 5.0 software was used for CFD calculations with a laminar and incompressible flow assumption. In previous studies, laminar calculations have been found to be suitable for nasal airflow. Uniform total pressure condition was applied in the nostrils. To study the airflow in the nasal cavities, we used a constant inspiratory flow rate that was also patient specific by determining the flow rate as a function of gender and weight (Garcia et al., 2009)

$$\begin{aligned} &\text{For } males := \dot{V}(1.36 \pm 0.10)M^{(0.44\pm0.02)} \\ &\text{For females} : \dot{V} = (1.89 \pm 0.40)M^{(0.32\pm0.06)} \end{aligned} \quad (1)$$

where $\dot{V}$ is flow rate (litres per minute) and M is weight in kilograms. Steady-state inspiratory flow rates used in the calculations were twice the mean flow rate for each patient defined from Eq. (1). In addition, equal flow rates were used pre- and postoperatively for each patient. All calculations were conducted with heat transfer from the rigid walls with no-slip condition. Ambient air had a temperature of 20 °C. For our heat transfer calculations, the mucous membrane surface temperatures T_{mucous} were adjusted to have a mean temperature of approximately 32 °C according to the following Equation:

$$\mathrm{q} = \mathrm{h}_m\left(T_{\text{body}} - T_{\text{mucous}}\right) \quad (2)$$

where q is a local heat flux (W/m^2) from the mucous membrane surface to airflow; T_{body} is body temperature of 310.15 Kelvin (K); T_{mucous} is a local mucous membrane surface temperature and h_m is a uniform heat transfer coefficient across the mucous membrane in all positions of the nasal cavities. Coefficient h_m was experimentally adjusted to $50W/\left(m^2K\right)$ to have similar mucous membrane surface temperatures as in the clinical measurements by Lindemann et al. (2002). Across the whole nasal cavity, Eq. (2) obtains approximately a mean mucous membrane surface temperature of 32 °C. When no local heat transfer is present, Eq.

Table 1
Patient selection and group information. Volumetric (vol.) measurements are from the air space surrounding the anterior 5–20 mm of the inferior turbinates.

	Patient selection and information by groups							
	Group 1 VAS change large Vol. change large		Group 2 VAS change large Vol. change small		Group 3 VAS change small Vol. change large		Group 4 VAS change small Vol. change small	
	Patient 1	Patient 2	Patient 3	Patient 4	Patient 5	Patient 6	Patient 7	Patient 8
Pre-vol. (mm^3)	1914	1118	4335	2238	2563	2085	2142	3330
Post-vol. (mm^3)	5949	3416	3879	2657	4881	4575	2073	3330
Vol. change	4035	2298	-456	419	2318	2490	-69	0
pre-VAS	8.0	8.0	8.0	8.0	7.0	10.0	6.0	8.0
post-VAS	2.0	0.0	0.0	1.0	4.0	7.0	3.0	7.0
VAS change	-6.0	-8.0	-8.0	-7.0	-3.0	-3.0	-3.0	-1.0
Sex	Female	Male	Male	Male	Female	Female	Male	Female
Weight	74	96	126	95	58	54	92	54
Flow rate (l/min)	15.0	20.3	22.8	20.2	13.9	13.5	19.9	13.5

(2) obtains a mucous membrane temperature of 37 °C. To complete the calculation of a single 3D model, one week was required with 24 processors.

2.3. Data analysis

In order to assess patients' local sensitivity to pressure losses, we calculated the mean pressure loss from the nostrils to the mean pressure along the whole surface of the inferior turbinates from the CFD calculations (Fig. 1). Then, total heat transfer was calculated in the operated anterior 25 mm of the interior turbinates. Furthermore, total pressure loss and total heat transfer from the nostrils to the nasopharynx were calculated to assess the total effects of the inferior turbinate surgeries. Nasopharynx results were measured vertically at the bottom level of inferior turbinates airways since not all patients had much downstream geometry from the nasopharynx. In all our cases, however, mesh geometry was extended 50 mm downstream from the nasopharynx for computational reasons. The analysis was made to both sides of the nasal cavities simultaneously as was the treatment and patient VAS assessment. The Wilcoxon signed-rank test was used to analyse the statistical significance of the results. The numerical post-processing of the acquired CFD data was made with the open source visualization and data analysis software ParaView 5.0.1.

3. Results

In the anterior 25 mm of the inferior turbinate, the median heat transfer postoperatively was less in all groups, except for Group 4 which had small VAS and volumetric changes. Preoperatively, the median heat transfer from the anterior 0–25 mm of the inferior turbinates for all 8 patients was 0.91 Watts (W), whereas the median heat transfer postoperatively was 0.65 W. The changes between preoperative and postoperative heat transfer for all eight patients were statistically significant ($p < 0.05$). This was the direct result of the enlarged postoperative airway volumes in those regions. (Table 2).

The median air temperatures in the nasopharynx postoperatively were also less in all groups, except for Group 4. The median air temperature in the nasopharynx for all 8 patients was 31.1 °C preoperatively and 30.9 °C postoperatively. (Table 3) The median pressure losses from ambient to inferior turbinates as well as to the nasopharynx were postoperatively less in Groups 1 and 3, which had large volumetric changes. However, the opposite was true for Groups 2 and 4, which had small volumetric changes. (Tables 4–5) The preoperative mucosal heat fluxes and pressure results are visually presented for Patient 1 (Figs. 2–3).

4. Discussion

In this study, we have presented the CFD results from a subset of inferior turbinate surgeries both preoperatively- and at twelve months postoperatively. Our results showed statistically significant reduced heat transfer in the anterior 25 mm of the inferior turbinates postoperatively. Similarly, several virtual studies of turbinate surgery have shown decreased total heat transfer in most cases (Lee et al., 2016; Na et al., 2012). We are unaware of previous studies with patients that have reported reduced heat transfer results for inferior turbinate surgery pre- and postoperatively. Previously, CFD studies have been reported after concomitant septorhinoplasty or septoplasty and turbinate surgery in patients with turbinate hypertrophy and septum deviation. Casey et al. (2017) examined preoperative patients and healthy controls but did not evaluate the effects of the surgical procedure. In their study, they found that healthy subjects had a significantly higher middle airflow than preoperative patients on the most obstructed side. Sullivan et al. (2014) conducted a study pre- and postoperatively without healthy controls. They found that a surface area where heat flux exceeds 50 W/m^2 on the obstructed side correlated best with VAS and NOSE survey results. Kimbell et al. (2013) reported pre- and postoperative CFD results for those patients who did not have nasal cycle effects in CT images. By contrast, Gaberino et al. (2017) studied patients with nasal cycle effects pre- and postoperatively. Nasal cycle effects were corrected computationally and correlations between CFD variables and subjective scores improved.

All the above-mentioned studies assessed VAS results unilaterally and mostly compared CFD results from the more obstructed side to the corresponding unilateral instantaneous VAS or longer-term NOSE survey results. This can be understood to be the most meaningful comparison since many patients were operated with septoplasty. Our patients underwent treatment in the anterior parts of the inferior turbinates on both sides. Similarly, VAS assessment from the previous seven days was made simultaneously on both sides. The choice of correct VAS

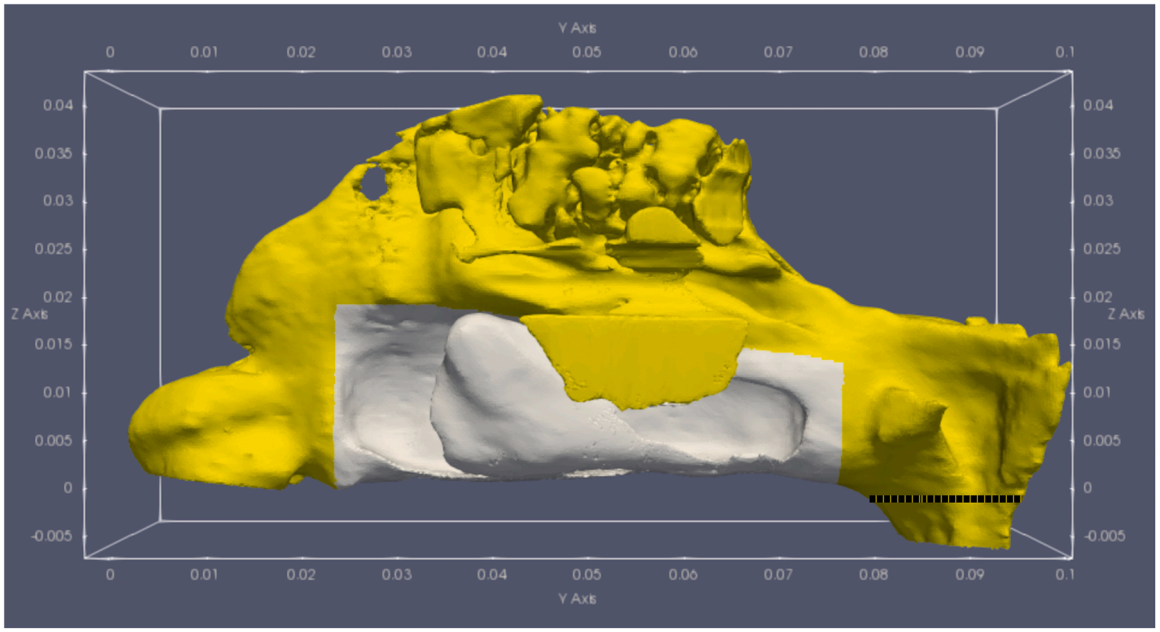

Fig. 1. The preoperative nasal cavities of Patient 1. Inferior turbinate regions are marked in white. Nasopharynx measurement position is marked with crosslines.

Table 2
Heat transfer from the mucosa of inferior turbinates 0–25 mm. The temperature of the inspired ambient air was 20 °C. The statistical significance of the change between pre- and postoperative results was analysed with Wilcoxon signed-rank test.

	Heat transfer inferior turbinates 0–25 mm				
	Group 1 VAS change large Vol. change large Patient 1 | Patient 2	Group 2 VAS change large Vol. change small Patient 3 | Patient 4	Group 3 VAS change small Vol. change large Patient 5 | Patient 6	Group 4 VAS change small Vol. change small Patient 7 | Patient 8	All patients
	Median	Median	Median	Median	Median
Pre [W]	0.82 | 0.99 0.91	0.76 | 1.28 1.02	1.02 | 0.57 0.79	0.99 | 0.75 0.87	0.91
Post [W]	0.46 | 0.68 0.57	0.64 | 0.55 0.59	0.65 | 0.41 0.53	1.07 | 0.75 0.91	0.65
Change [W]	-0.36 | − 0.31 -0.34	-0.12 | − 0.73 -0.42	-0.37 | − 0.16 -0.27	0.08 | 0.00 0.04	-0.23 ($p < 0.05$)
Post/Pre	0.56 | 0.69 0.62	0.84 | 0.43 0.64	0.64 | 0.72 0.68	1.08 | 1.00 1.04	–

Table 3
Air temperature at nasopharynx and total nasal heat transfer from nostrils to nasopharynx. The temperature of the inspired ambient air was 20 °C. The statistical significance of the change between pre- and postoperative results was analysed with Wilcoxon signed-rank test.

	Air temperature at nasopharynx and total heat transfer				
	Group 1 VAS change large Vol. change large Patient 1 | Patient 2	Group 2 VAS change large Vol. change small Patient 3 | Patient 4	Group 3 VAS change small Vol. change large Patient 5 | Patient 6	Group 4 VAS change small Vol. change small Patient 7 | Patient 8	All patients
	Median	Median	Median	Median	Median
Pre air temperature at nasopharynx [°C]	33.0 | 30.5 31.8	30.7 | 30.6 30.7	34.6 | 31.7 33.1	29.6 | 31.5 30.6	31.1
Post air temperature at nasopharynx [°C]	30.4 | 31.3 30.9	30.4 | 28.2 29.3	32.0 | 30.7 31.3	31.0 | 31.1 31.1	30.9
Air temperature change at nasopharynx [°C]	-2.6 | 0.8 -0.9	-0.3 | − 2.4 -1.4	-2.6 | − 1.0 -1.8	1.4 | − 0.4 0.5	-0.7 ($p = 0.18$)
Preoperative total heat transfer [W]	3.90 | 4.26 4.08	4.88 | 4.28 4.58	4.06 | 3.16 3.61	3.82 | 3.10 3.46	3.98
Postoperative total heat transfer [W]	3.12 | 4.59 3.86	4.74 | 3.31 4.03	3.33 | 2.89 3.11	4.38 | 3.00 3.69	3.32
Post/Pre Total heat transfer	0.80 | 1.08 0.94	0.97 | 0.77 0.87	0.82 | 0.91 0.87	1.15 | 0.97 1.06	–

assessment remains challenging since many factors can affect the instantaneous and longer-term subjective feelings of nasal patency.

The median heat transfer in the anterior 25 mm of the inferior turbinates only increased in the group with small volumetric and small VAS changes and decreased in all the other groups. Heat transfer results were in line with VAS changes. However, no statistical analysis was performed due to the small sample size. This resulted mostly from larger air volumes in regions that reduce heat transfer. In the total heat transfer results, the ratios of changes between pre- and postoperative conditions were smaller than in the heat transfer results from the anterior parts of the inferior turbinates. This result stems from the inferior turbinate heat transfer only contributing to a part of the total nasal heat transfer. Furthermore, the procedure also causes redivision of the heat transfer in the nasal cavity. Smaller heat transfer in the anterior parts leads to higher heat transfer in the posterior parts, which, in turn, stems from colder air flowing downstream in the nasal cavities.

For pressure losses, local pressure at the inferior turbinates and across the whole nasal cavities alike, groups with large volumetric changes had smaller median pressure losses postoperatively, whereas for groups with small volumetric changes the opposite was true (Tables 4–5). Pressure loss results did not correlate with VAS changes. However, it could be assumed that pressure losses would be smaller after inferior turbinate surgery for larger cohorts since the increase of volume leads to smaller pressure losses, as happens in more simplified structures. In previous studies, strong correlations between sinus pathologies (Valtonen et al., 2018) or rhinomanometric results (André et al., 2009) and the patients' subjective assessment have not been found.

Calculated heat transfer is subject to assumptions about nasal

Table 4
Pressure difference from ambient to nasopharynx. The statistical significance of the change between pre- and postoperative results was analysed with Wilcoxon signed-rank test.

	Pressure difference from ambient to nasopharynx				
	Group 1 VAS change large Vol. change large	Group 2 VAS change large Vol. change small	Group 3 VAS change small Vol. change large	Group 4 VAS change small Vol. change small	All patients
	Patient 1 | Patient 2	Patient 3 | Patient 4	Patient 5 | Patient 6	Patient 7 | Patient 8	
	Median	Median	Median	Median	Median
Pre [Pa]	20.0 | 128.7	19.9 | 41.4	22.9 | 12.0	34.1 | 7.7	21.5
	74.4	30.7	17.4	20.9	
Post [Pa]	6.6 | 19.0	21.6 | 53.8	12.2 | 11.6	54.2 | 9.5	15.6
	12.8	37.7	11.9	31.9	
Change [Pa]	-13.4 | − 109.7	1.7 | 12.4	-10.7 | − 0.4	20.1 | 1.8	0.6 (p = 0.94)
	-61.5	7.0	-5.5	11.0	
Post/Pre	0.33 | 0.15	1.09 | 1.30	0.53 | 0.97	1.59 | 1.23	–
	0.24	1.19	0.75	1.41	

Table 5
Pressure difference from ambient to area-averaged mean pressure at inferior turbinates. The statistical significance of the change between pre- and postoperative results was analysed with Wilcoxon signed-rank test.

	Pressure difference from ambient to mean pressure at inferior turbinates				
	Group 1 VAS change large Vol. change large	Group 2 VAS change large Vol. change small	Group 3 VAS change small Vol. change large	Group 4 VAS change small Vol. change small	All patients
	Patient 1 | Patient 2	Patient 3 | Patient 4	Patient 5 | Patient 6	Patient 7 | Patient 8	
	Median	Median	Median	Median	Median
Pre [Pa]	14.7 | 103.0	17.9 | 22.0	17.6 | 11.7	29.2 | 6.2	17.8
	58.8	20.0	14.6	17.7	
Post [Pa]	5.9 | 16.2	21.2 | 38.3	10.4 | 11.5	35.8 | 7.2	13.9
	11.0	29.8	10.9	21.5	
Change [Pa]	-8.8 | − 86.8	3.3 | 16.3	-7.2 | − 0.2	6.6 | 1.0	0.4 (p = 0.84)
	-47.8	9.8	-3.7	3.8	
Post/Pre	0.40 | 0.16	1.18 | 1.74	0.59 | 0.98	1.23 | 1.16	–
	0.28	1.46	0.79	1.19	

mucosal temperatures. We approached these calculations by not assuming a constant mucous membrane temperature along the nasal cavity, but by varying nasal mucosal temperatures as a function of heat transfer itself (Eq. 2). An example of this is visually presented (Fig. 4). This approach was a numerical fit to the experimental mucosal temperatures along the nasal cavity (Lindemann et al., 2002). In their study, Lindemann et al. measured statistically different mucosal temperatures along the nasal cavity. Furthermore, our approach assumes that mucosal temperature is 37 °C while local heat transfer from the mucous membrane is not present. Unfortunately, temperature data are very scarce along the nasal cavity and few studies have been made. Further, areas with negligible heat transfer are hard to measure. It could be that our assumption is not completely true either and results in too much variation in nasal mucosal temperatures along the nasal cavities. Except for Na et al. (2012), other studies have mostly used constant mucous membrane surface temperatures. Although further studies with larger datasets will probably improve nasal mucosal temperature calculations but may have a similar form as our Eq. 2.

Our results assume that inspiratory flow rates are independent from surgery volumetric changes and that patients breathe as much pre- and postoperatively as corresponding healthy individuals. It can be expected that this assumption holds true for a large majority of patients. However, some studies have assumed that postoperative pressure loss was equal to the preoperative pressure loss which resulted in reduced flow rates preoperatively (Kimbell et al., 2013; Sullivan et al., 2014; Gaberino et al., 2017).

Our assumption was that the heat transfer properties of mucous membrane are exactly the same pre- and postoperatively. Heat transfer in the anterior part of the inferior turbinate was less postoperatively than preoperatively which is to be expected when air volumes become greater and flow gradients at the mucous membrane surfaces are reduced. The median total heat transfer also decreased in almost all investigated groups. Additionally, reduced postoperative heat transfer at the anterior parts led to increased heat transfer at the posterior parts of the nasal cavities. At the same time, VAS scores were better postoperatively. These results could support the hypothesis that certain receptors that are sensitive to nasal congestion are concentrated more on the posterior parts of the nasal cavity or even the nasopharynx. In the

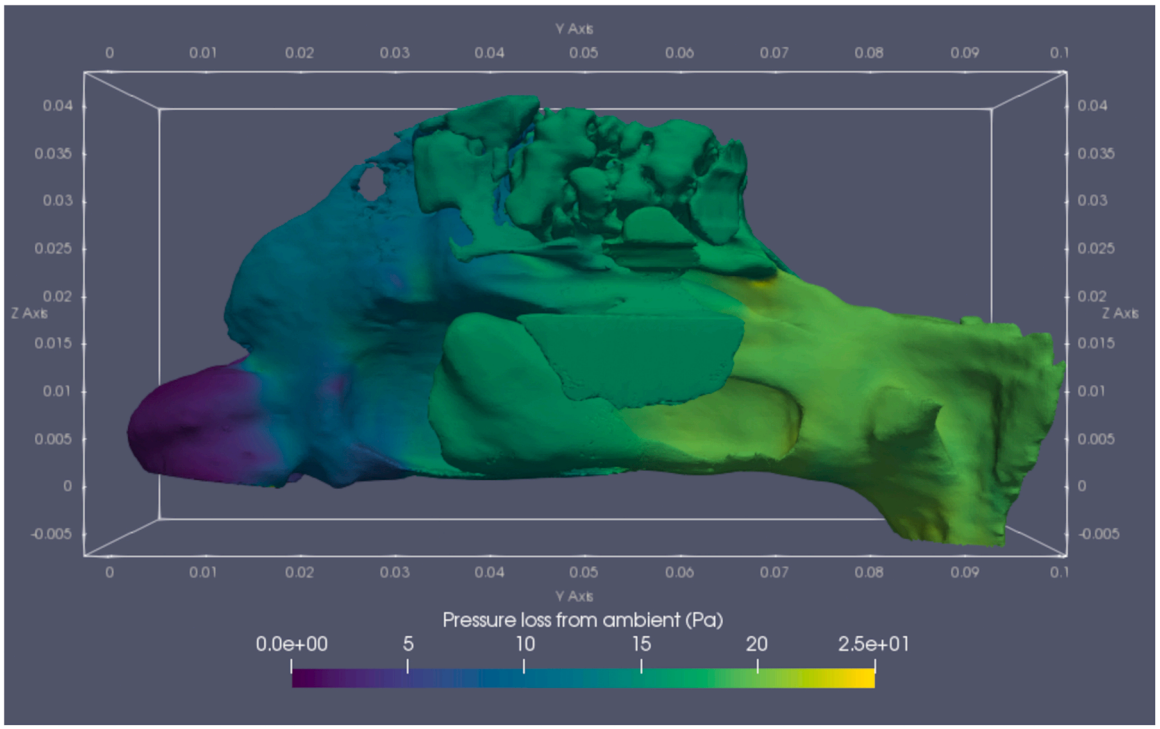

Fig. 2. The preoperative pressure loss (Pa) results from ambient to the nasal mucosa for Patient 1.

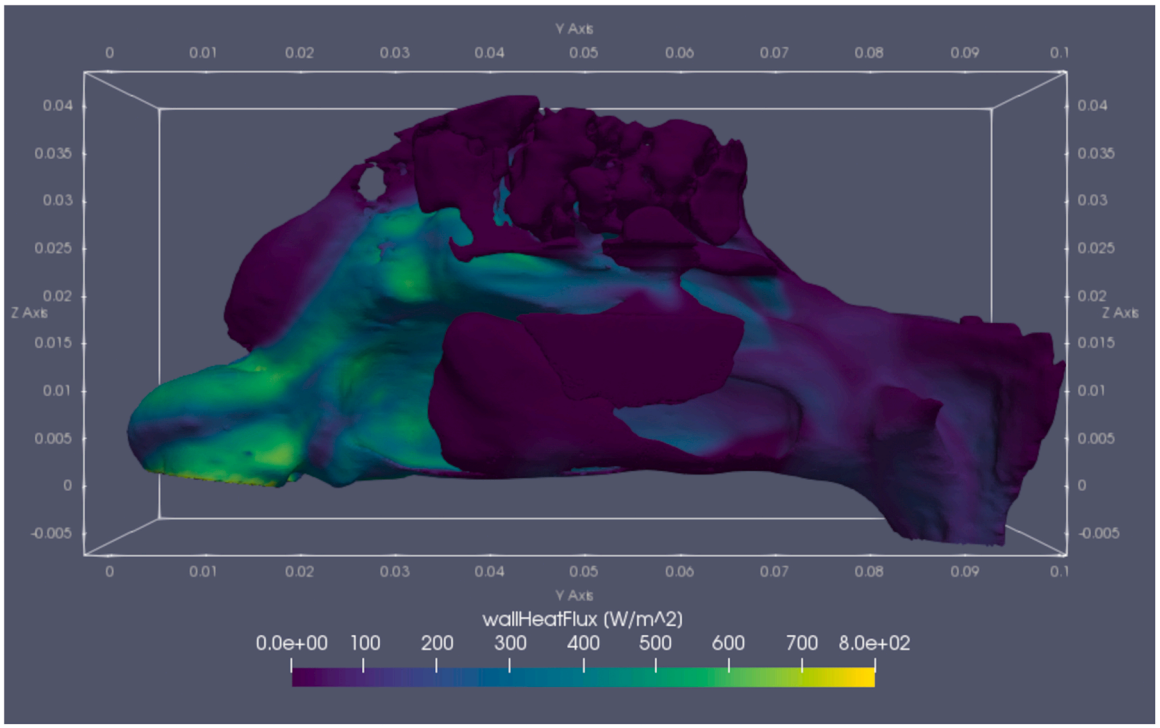

Fig. 3. The preoperative nasal mucosa heat fluxes (W/m^2) for Patient 1.

previous literature, Meusel et al. (2010) reported the uniform distribution of menthol-sensitive receptors in the nasal cavity. In future studies, one possibility could be to include the modelling of mucous membrane properties coupled with CFD calculations.

This study presents a patient series with clinically homogenic inferior turbinate hypertrophy, and all other nasal diseases were excluded. Radiological heterogeneity in a geometric variation of the nasal cavities exists among our patients and within our study groups, as it does generally in all populations. Therefore, it is very important that the results of surgery are evaluated between pre- and postoperative scans of the same patient.

The limitations of the study are the small sample size and the preliminary nature of the study. In the groups with small volumetric changes in the anterior parts of the inferior turbinates, small overall

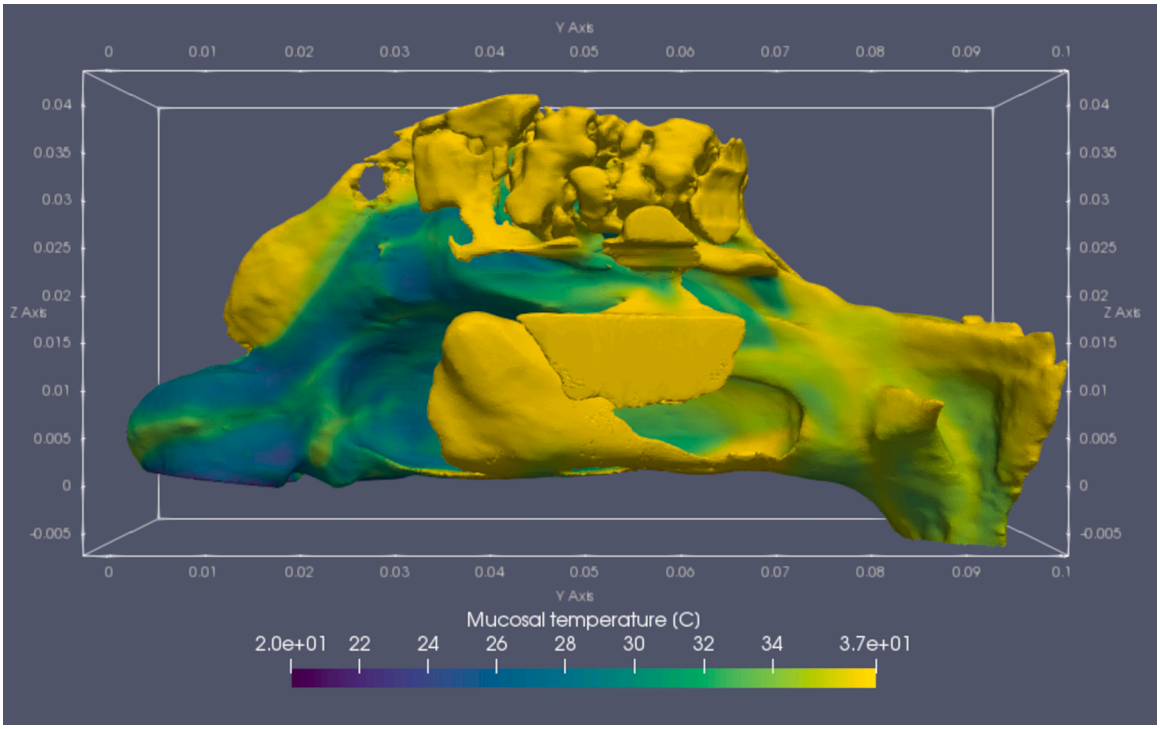

Fig. 4. The preoperative nasal mucosal temperatures (°C) for Patient 1.

contractions of the nasal cavities might be possible postoperatively and may have had a slight effect on the pressure drop results, as was the case at 12-month follow-up in the present study. In future, better surgical planning could enhance surgical operations and unexpected results would become less common.

In future studies, larger patients cohorts will be needed. However, in these studies, many regional CFD results along the nasal cavities often correlate strongly with other regions in close proximity. Thus, this makes a localized psychophysical model of patient well-being as a function of flow quantities hard to develop. One solution could be to assume that local sensitivity to airflow quantities is uniform in large parts of the nasal cavities. One could even assume VAS and Quality of life (QOL) results are a function weighted sum of flow variables at certain regions of the nasal cavities. The method used in the present study can obtain CFD results that reveal changes in flow quantities due to inferior turbinate surgery. Therefore, our presented method can be used for assessing larger cohorts of patients and for developing psychophysical models of nasal congestion.

Currently, the information obtained from CBCT scans is not used to its full extent in clinical practice. In most cases, CBCT scans are used in the examination of patients with chronic rhinosinusitis. The information provided by CBCT scans can, however, be used in CFD calculations to comprehensively study nasal airflow in the nasal cavities. The results of the present study demonstrate that CFD can assess differences in airflow quantities as a result of volumetric changes due to inferior turbinate surgery. These methods provide future possibilities for assessing nasal congestion and its effect on the well-being of patients.

5. Conclusions

Surgical interventions reduced heat transfer in the operated parts of the inferior turbinates and were in line with patient VAS changes. This study shows that CFD is an option in assessing patient well-being as a function of airflow parameters from mucous membrane with larger data sets. The results support the hypothesis that nasal congestion – sensitive receptors might be more concentrated at the posterior parts of the nasal cavities. CFD could therefore have potential in the planning and evaluation of nasal surgical procedures in future. The limitations of the study are the small sample size and the preliminary nature of the study.

Conflict of Interest Statement

The authors declare that there is no conflict of interest.

Acknowledgement

The author(s) received financial support from the Finnish ORL-HNS Foundation, Finland' and Tampere Tuberculosis Foundation, Finland' for the research, authorship, and/or publication of this article.

References

André, R.F., Vuyk, H.D., Ahmed, A., Graamans, K., Nolst Trenité, G.J., 2009. Correlation between subjective and objective evaluation of the nasal airway. A systematic review of the highest level of evidence. Clin. Otolaryngol. 34 (6), 518–525. https://doi.org/10.1111/j.1749-4486.2009.02042.x.

Casey, K.P., Borojeni, A.A.T., Koenig, L.J., Rhee, J.S., Garcia, G.J.M., 2017. Correlation between subjective nasal patency and intranasal airflow distribution. Otolaryngol. Head Neck Surg. 156 (4), 741–750. https://doi.org/10.1177/0194599816687751.

Gaberino, C., Rhee, J.S., Garcia, G.J.M., 2017. Estimates of nasal airflow at the nasal cycle mid-point improve the correlation between objective and subjective measures of nasal patency. Respir. Physiol. Neurobiol. 238, 23–32. https://doi.org/10.1016/j.resp.2017.01.004.

Garcia, G.J.M., Schroeter, J.D., Segal, R.A., Stanek, J., Foureman, G.L., Kimbell, J.S., 2009. Dosimetry of nasal uptake of water-soluble and reactive gases: a first study of interhuman variability. Inhal. Toxicol. 21 (7), 607–618. https://doi.org/10.1080/08958370802320186.

Harju, T., Numminen, J., Kivekäs, I., Rautiainen, M., 2018. A prospective, randomized, placebo-controlled study of inferior turbinate surgery. Laryngoscope 128 (9), 1997–2003. https://doi.org/10.1002/lary.27103.

Kim, S.K., Na, Y., Kim, J.-I., Chung, S.-K., 2013. Patient specific CFD models of nasal airflow: overview of methods and challenges. J. Biomech. 46 (2), 299–306. https://doi.org/10.1016/j.jbiomech.2012.11.022.

Kimbell, J.S., Frank, D.O., Laud, P., Garcia, G.J.M., Rhee, J.S., 2013. Changes in nasal airflow and heat transfer correlate with symptom improvement after surgery for nasal obstruction. J. Biomech. 46 (15), 2634–2643. https://doi.org/10.1016/j.jbiomech.2013.08.007.

Lee, K.B., Jeon, Y.S., Chung, S.K., Kim, S.K., 2016. Effects of partial middle turbinectomy with varying resection volume and location on nasal functions and airflow characteristics by CFD. Comput. Biol. Med. 77, 214–221. https://doi.org/10.1016/j.compbiomed.2016.08.014.

Lindemann, J., Leiacker, R., Rettinger, G., Keck, T., 2002. Nasal mucosal temperature during respiration. Clin. Otolaryngol. Allied Sci. 27 (3), 135–139. https://doi.org/10.1046/j.1365-2273.2002.00544.x.

Meusel, T., Negoias, S., Scheibe, M., Hummel, T., 2010. Topographical differences in distribution and responsiveness of trigeminal sensitivity within the human nasal mucosa. Pain 151 (2), 516–521. https://doi.org/10.1016/j.pain.2010.08.013.

Na, Y., Chung, K.S., Chung, S.K., Kim, S.K., 2012. Effects of single-sided inferior turbinectomy on nasal function and airflow characteristics. Respir. Physiol. Neurobiol. 180 (2–3), 289–297. https://doi.org/10.1016/j.resp.2011.12.005.

Ormiskangas, J., Valtonen, O., Kivekäs, I., Dean, M., Poe, D., Järnstedt, J., Lekkala, J., Harju, T., Saarenrinne, P., Rautiainen, M., 2020. Assessment of PIV performance in validating CFD models from nasal cavity CBCT scans. Respir. Physiol. Neurobiol. 282, 103508 https://doi.org/10.1016/j.resp.2020.103508.

Quadrio, M., Pipolo, C., Corti, S., Lenzi, R., Messina, F., Pesci, C., Felisati, G., 2014. Review of computational fluid dynamics in the assessment of nasal air flow and analysis of its limitations. Eur. Arch. Otorhinolaryngol. 271 (9), 2349–2354. https://doi.org/10.1007/s00405-013-2742-3.

Radulesco, T., Meister, L., Bouchet, G., Giordano, J., Dessi, P., Perrier, P., Michel, J., 2019. Functional relevance of computational fluid dynamics in the field of nasal obstruction: a literature review. Clin. Otolaryngol. 44 (5), 801–809. https://doi.org/10.1111/coa.13396.

Sullivan, C.D., Garcia, G.J.M., Frank-Ito, D.O., Kimbell, J.S., Rhee, J.S., 2014. Perception of better nasal patency correlates with increased mucosal cooling after surgery for nasal obstruction. Otolaryngol. Head Neck Surg. 150 (1), 139–147. https://doi.org/10.1177/0194599813509776.

Valtonen, O., Bizaki, A., Kivekäs, I., Rautiainen, M., 2018. Three-dimensional volumetric evaluation of the maxillary sinuses in chronic rhinosinusitis surgery. Ann. Otol. Rhinol. Laryngol. 127 (12), 931–936. https://doi.org/10.1177/0003489418801386.

Valtonen, O., Ormiskangas, J., Kivekäs, I., Rantanen, V., Dean, M., Poe, D., Järnstedt, J., Lekkala, J., Saarenrinne, P., Rautiainen, M., 2020. Three-dimensional printing of the nasal cavities for clinical experiments. Sci. Rep. 10, 502. https://doi.org/10.1038/s41598-020-57537-2.

Valtonen, O., Ormiskangas, J., Harju, T., Rautiainen, M., Kivekäs, I., 2021. Three-dimensional measurements in assessing the results of inferior turbinate surgery. Ann. Otol. Rhinol. Laryngol. https://doi.org/10.1177/00034894211028516.

Vogt, K., Jalowayski, A.A., Althaus, W., Cao, C., Han, D., Hasse, W., Hoffrichter, H., Mösges, R., Pallanch, J., Shah-Hosseini, K., Peksis, K., Wernecke, K.D., Zhang, L., Zaporoshenko, P., 2010. 4-Phase-rhinomanometry (4PR)–basics and practice 2010. Rhinol. Suppl. 21, 1–50.

Zubair, M., Abdullah, M.Z., Ismail, R., Shuaib, I., Hamid, S.A., Ahmad, K.A., 2012. Review: a critical overview of limitations of cfd modeling in nasal airflow. J. Med. Biol. Eng. 32 (2), 77–84. https://doi.org/10.5405/jmbe.948.